Analytical Methods

Accepted Manuscript

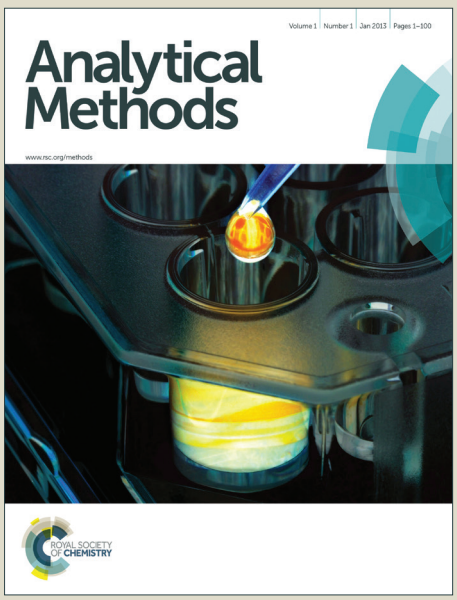

ROYAL SOCIETY OF CHEMISTRY

www.rsc.org/methods

Quantitative analysis of the water of crystallization of gypsum by near-infrared spectroscopy in Yungang Grottoes

Yang Zhao[a,b] Meiying Li[a,b] Xia Wei[a,b] Xinyu Shen[a,b] Feng Gao[c] Hua Tong[a,b,*]

[a]College of Chemistry and Molecular Sciences, Wuhan University, Wuhan 430072, China

[b]Archaeology Research Center of Science and Technology, Wuhan University, Wuhan 430072, China

[c]Chinese Academy of Cultural Heritage, Beijing 100029, China

*sem@whu.edu.cn

Abstract: Near infrared spectroscopy is considered to be an effective analytical tool which is used in various fields, however, it is rarely used in the analysis of water of crystallization of rocks on the stone relics. In the present study, calibration model was developed for non-destructive estimation of water of crystallization content of dihydrate gypsum in the rocks by fourier transform near infrared spectroscopy. A total of 51 samples were prepared in the laboratory to simulate the actual samples from Yungang Grottoes, their fourier transform near infrared spectra were correlated to water of crystallization content by means of partial least square regression, and then calibration model was developed. The 5 actual samples from Yungang Grottoes were analyzed by X-ray diffraction and X-ray fluorescence. The optimal model was achieved with the correlation coefficient of 0.9899 and the root mean square error of cross validation of 0.2190, and the correlation coefficient and the root mean square error of prediction of the validation set were 0.9834 and 0.4558, respectively.

Keywords: Near infrared spectroscopy; Partial least square; Dihydrate gypsum; Quantitative analysis; In situ measurement.

1 Introduction

Yungang Grottoes (A.D. 460-524) have a very significant position in the history of Chinese sculpture art. In recent years, the weathering of rocks in the grottoes is getting more and more serious.[1-3] Water of crystallization content of minerals is an important factor for the weathering of these rocks. In Yungang Grottoes, the main ingredient is kaolin, in addition, sulfur element can be detected in the actual samples. Obviously, sulfur element mainly comes from the surrounding environment where an industrial city is. The sulfur element is found that it exists in the form of gypsum by X-ray diffraction (XRD). It has been reported that gypsum is formed by sulfite hemihydrate.[4, 5] Some minerals reacting with water will turn water into one of their components, thus these new kinds of compounds generate.[6] Such minerals are defined as precipitated salt. Gypsum is the typical representative of the type minerals, which can absorb a certain amount of water to form dihydrate gypsum (Fig. 1). The swelling of rocks after absorbing water not only lead to volume dilatation, but also create pressure on the surrounding rocks.[7-12] As a result, stone relics will suffer from the dangers of cracking. Therefore, it is significant to detect water of crystallization content of gypsum on the scene in Yungang Grottoes.

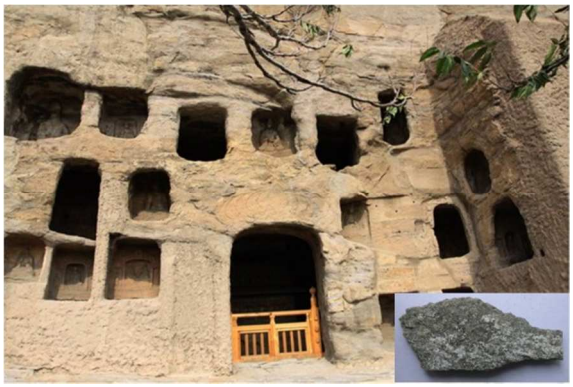

Fig. 1. Cave 39 of Yungang Grottoes

Near infrared (NIR) spectroscopy combined with chemometrics has been proved to be an easy, convenient and non-destructive quantitative technology for components of complex samples.[13-17] Its region is a part of the electromagnetic spectrum between the microwave and the visible wavelength, related to vibration and combination overtones of the C-H, N-H, O-H and S-H bonds.[18, 19] Therefore, NIR has been widely used in the fields of foodstuffs,[20, 21] tobaccos,[22, 23] agriculture,[24-26] medicines,[27, 28] biological tissues,[29-31] polymers[32] and petrochemical products.[33, 34] In the field of mineralogy, the NIR has been used to detect the presence of gypsum.[35, 36] However, it is rarely reported that NIR has been applied to determine the water of crystallization content of minerals on the stone relics. Due to the characteristic of non-destructive analysis of NIR, this method is very suitable for detecting stone relics in situ.

In this paper, the water of crystallization content of gypsum from Yungang Grottoes has been determined by NIR. It is the first time to use non-destructive quantitative technology of NIR to analyze the precipitated salt in situ. Fresh rocks without gypsum around Yungang Grottoes were made into powders, and a different proportion of dihydrate gypsum was added to the powders. Then the powders were pressed into wafers as calibration samples of near infrared model, and the wafers were analyzed by NIR. Partial least squares (PLS) regression was used as algorithm of the model. The experimental results show that this model can be applied in the actual measurement. The near infrared spectrums of stone relics in Yungang Grottoes are achieved by portable near infrared spectrometer. When the near infrared spectra are imported into the near infrared model, the water of crystallization content of gypsum can be achieved immediately.

2 Experimental

2.1 Materials

Fresh rocks without gypsum were obtained around the Yungang Grottoes. Actual samples which were peeling rock fragments on the ground were collected from Cave 38 and 39 (A.D. 494-525) in Yungang Grottoes. Dihydrate gypsum ($CaSO_4 \cdot 2H_2O$, analytical purity grade) was purchased from

Sinopharm Chemical Reagent Co..

2.2 Chemical characterization of the 5 actual samples

The 5 actual samples were analyzed by using wide angle X-ray diffraction (XRD, X'pert PRO, Panalytical, Holland) and X-ray fluorescence (XRF, S4 PIONEER, Bruker AXS, Germany).

2.3 Laboratory samples preparation

Fresh rocks were ground into powders, and then the powders were divided into 51 groups. A certain mass of dihydrate gypsum was added to the powders according to the quality ratios of water of crystallization of 0.1%, 0.2%, 0.3% ... 5.0%, 5.1%, respectively. Fresh rocks and dihydrate gypsum were mixed homogeneously by oscillating mixer (Shimadzu, Japan). Then the mixed powders pressed into wafers were prepared for near-infrared spectral acquisition.

2.4 NIR spectral measurement

The spectra of the actual samples were recorded by using a FTNIR spectrometer (TerraSpec 4 St-Res, ASD, USA) which was a portable instrument. The spectra could be obtained in situ when the NIR probe gently pressed on the actual sample surface. All the NIR spectra were collected from

350 to 2500 nm in diffuse reflectance mode. The FTNIR spectrometer collected spectra of samples at 10 nm interval. To increase SNR (signal to noise ratio), both actual samples and laboratory samples were scanned 32 times by FTNIR spectrometer，and each spectrum was averaged from three parallel measurements. The temperature and relative humidity were maintained at 25ºC and 40%, respectively.

2.5 PLS modeling

The NIR model of the water of crystallization content of dihydrate gypsum was performed with the software package TQ Analyst (thermo, USA). 51 laboratory samples were taken as calibration set for building the PLS model, the 5 actual samples which were collected from Cave 38 and 39 in Yungang Grottoes were used as validation set to test the practicability of the method.

The spectral datasets were correlated with water of crystallization content by using partial least squares regression algorithm. To evaluate the performance of the PLS regression model, the correlation coefficient (R) and root mean square error of cross validation (RMSECV) which were determined by leave-one-out cross validation (LOO-CV) were used. The RMSECV was the prediction error of a calibration model, and it was defined as the standard deviation between spectral data and reference values in the cross-validation

sample set. The value provides the average uncertainty that can be used for predictions of unknown samples, so an optimum model is based on minimum value of RMSECV. The factor number for PLS model was also determined by using LOO-CV with F-test. In addition, the optimization of PLS model needed to avoid the influence of drifting baseline and background in the spectra by using multiplicative signal correction (MSC) and derivative calculation. The outliers of PLS model were removed by using mahalanobis distance. For the validation set, correlation coefficient (R) and root mean square error of prediction (RMSEP) between the reference and prediction content were used to estimate the prediction of the developed model.

3 Results and discussion

3.1 Chemical analysis of the actual samples

The XRD pattern of the actual sample was used to investigate the compound form of sulfur element existing in the rocks of Yungang Grottoes. As shown in Fig. 2, the rocks of Yungang Grottoes were mainly composed of kaolin, and the diffraction peaks of dihydrate gypsum could also be found. The typical diffraction peaks of dihydrate gypsum were displayed with peaks at 30.7° and 33.7°in the XRD pattern, which represented crystal plane (200) and (220), respectively. Due to the low content of dihydrate gypsum, the intensity

of diffraction peaks was weak. So it could be concluded that sulfur element was present in the form of dihydrate gypsum in the rocks. By means of X-ray fluorescence (XRF), the content of sulfur element can be accurately determined. Then according to the chemical formula of dihydrate gypsum, the water of crystallization content of dihydrate gypsum can be also obtained. Table Ⅰ shows the water of crystallization content of 5 actual samples.

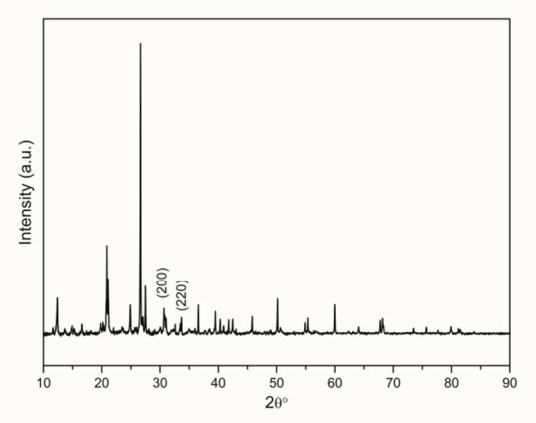

Fig. 2. XRD diffractogram of the actual sample from Yungang Grottoes

Table Ⅰ. The water of crystallization content of 5 actual samples obtained by the reference method

Samples	Sulfur element content (wt%)	Water of crystallization content (wt%)
Sample 1 from Cave 38	1.63	1.83
Sample 2 from Cave 38	2.24	2.52
Sample 3 from Cave 39	0.81	0.91
Sample 4 from Cave 39	0.47	0.53
Sample 5 from Cave 39	1.89	2.13

3.2 FTNIR spectra

The quantitative NIR model was built with "TQ Analyst" software package by using PLS regression. The selection of spectral regions that participated in the modeling was a method of data reduction. Analysis regions of the spectra which were too broad would lead to increase invalid information, and reduce the rate of effective information. Conversely, it would lead to the loss of useful information, and reduce the accuracy of the NIR model. In the study, 4458.62-5060.30cm^{-1} and 5106.58-5199.15cm^{-1} were selected to participate in the modeling. Generally, it was difficult to assign spectral regions to specific functional groups in the NIR. However, for the dihydrate gypsum, the two

spectral ranges were considered to be assigned to υ_s(OH)+δ(OH) and υ_a(OH)+δ(OH), respectively.[37] The spectral regions selected were considered to be the optimal option of the NIR model. Fig. 3 represents the spectra of the samples that were taken in the whole NIR range. Compared with the spectrum of the actual sample, the absorption bands in the spectrum of the laboratory sample were essentially the same with the actual sample, just showed differences from the actual sample in peak intensity. The laboratory sample could preferably simulate the actual sample. Therefore, it could be proved to be a feasible method for the determination of the water of crystallization content.

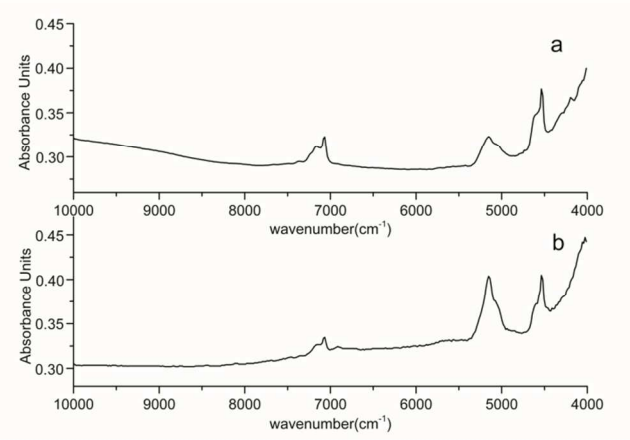

Fig. 3. The NIR spectra of the samples in the whole NIR range. (a) The actual sample from Yungang Grottoes. (b) The laboratory sample.

Spectral preprocessing methods including multiplicative signal correction (MSC) and derivative calculation for the NIR model were optimized by using

LOO-CV. In this process, different preprocessing methods were used to obtain the optimized NIR model. MSC could avoid the influence of inconstant optical path due to the non-uniformity of particles. Derivative calculation could remove drifting baseline, and separate overlapping information. Table Ⅱ summarizes the results that were obtained by using different preprocessing methods. According to both the correlation coefficient (R) and the root mean square error of cross validation (RMSECV), it could be found that MSC with first derivative could significantly improve the NIR model. Fig. 4 represents that the optimal factor number for the NIR model was found to be 3.

Table Ⅱ. NIR models and the results of cross-validation

Analyte	Preprocessing	Wavelength regions	R	RMSECV	Factor
water of crystallization	MSC	4458.62-5060.30cm^{-1} 5106.58-5199.15cm^{-1}	0.9531	0.3112	6
water of crystallization	MSC + first derivative	4458.62-5060.30cm^{-1} 5106.58-5199.15cm^{-1}	0.9899	0.2190	3
water of crystallization	MSC + second derivative	4458.62-5060.30cm^{-1} 5106.58-5199.15cm^{-1}	0.9727	0.2934	3

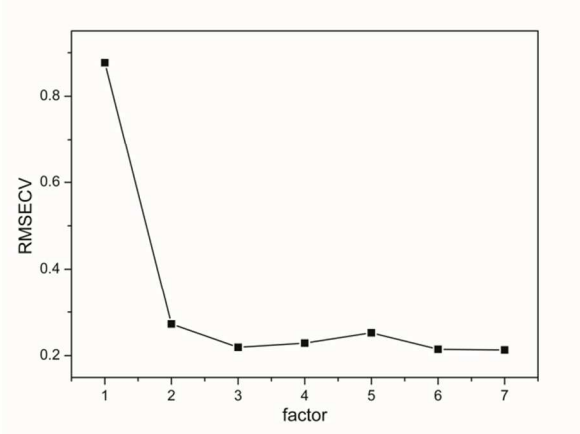

Fig. 4. Relationship between factor number and RMSECV

3.3 Removal of outliers

In the process of the modeling, the predictive accuracy of the model would greatly reduce when some samples were added to the model. Such samples were defined as outliers. It was obvious that the outliers were harmful to the NIR model. Therefore, the outliers should be removed by using mahalanobis distance. The mahalanobis distance showed the covariance distance of the data, it was an effective method to calculate the similarity of two unknown samples. The greater value of mahalanobis distance showed lower similarity. Fig. 5 shows that there were 6 outliers to be removed in the calibration set.

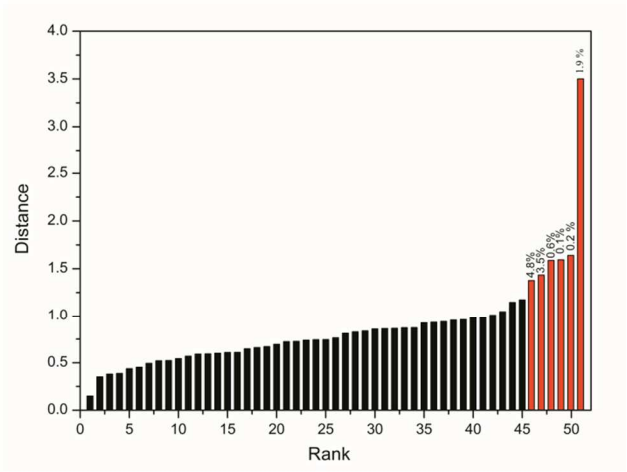

Fig. 5. Mahalanobis distances of the 51 laboratory samples

3.4 Quantitative model

The quantitative NIR model was built with the software package TQ Analyst. The wavelength regions, spectral preprocessing methods and factor numbers for the PLS calibration model was optimized combinatorially by using LOO-CV. 4458.62-5060.30cm^{-1} and 5106.58-5199.15cm^{-1} were considered to be the optimal option for the NIR model. From both the correlation coefficient (R) and the RMSECV in the table Ⅱ, MSC with first derivative was selected to preprocess the spectra. The optimal factor number for the NIR model was determined to be 3. Besides, there were 6 outliers to be removed by mahalanobis distance. Based on the above work, the correlation coefficient (R) and the RMSECV of the optimal model were found to be 0.9899 and 0.2190, respectively. The meaning of the value obtained from the

NIR model could be interpreted as the weight percentage of the water of crystallization in the rock in the measurement area.

3.5 Validation of the NIR model

In order to measure water of crystallization content of dihydrate gypsum, 45 laboratory samples were finally used to develop the calibration model and 5 actual samples were used as external samples to validate the NIR model. The developed calibration model using cross validation gave the correlation coefficient (R) was 0.9899, and RMSECV was 0.2190. Yungang Grottoes is the cultural heritage of world, so the 5 actual samples from Cave 38 and 39 are very precious. Then the optimized NIR model was used to predict the water of crystallization content of dihydrate gypsum in the actual samples. Fig. 6 shows the relationship between the predictive values and the reference values of the actual samples in the validation set. In the figure, the predictive values were predicted by the NIR model obtained above, and the reference values were from chemical test. It can be found that a good linearity was obtained in the content range of 0.3%-5.1%. With linear regression of these points, the correlation coefficient (R) and root mean square error of prediction (RMSEP) were found to be 0.9834 and 0.4558, respectively. However, a bias could be found in the fig. 6, this may be caused by random errors because there were

only 5 actual samples. If there were more actual samples to be used, the error may be corrected.

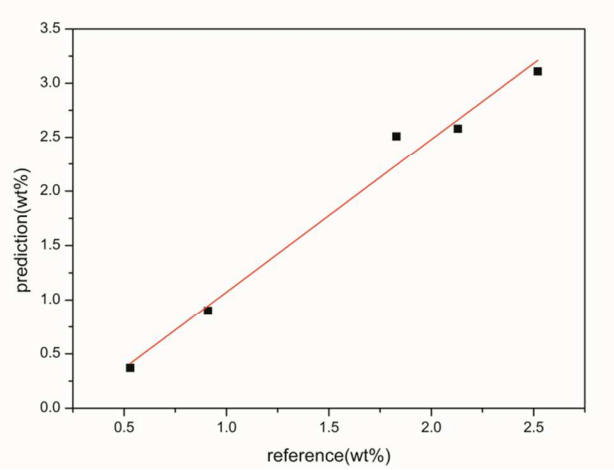

Fig. 6. Regression line of PLS model for the water of crystallization content of dihydrate gypsum obtained by FTNIR spectroscopy

In order to make up for the lack of the actual samples, some laboratory samples which were prepared according to random quality ratios were chosen as validation set. Fig. 7 shows the relationship between the predictive values and the reference values of these random laboratory samples. With linear regression of these points, the correlation coefficient (R) and root mean square error of prediction (RMSEP) were found to be 0.9779 and 0.3736, respectively.

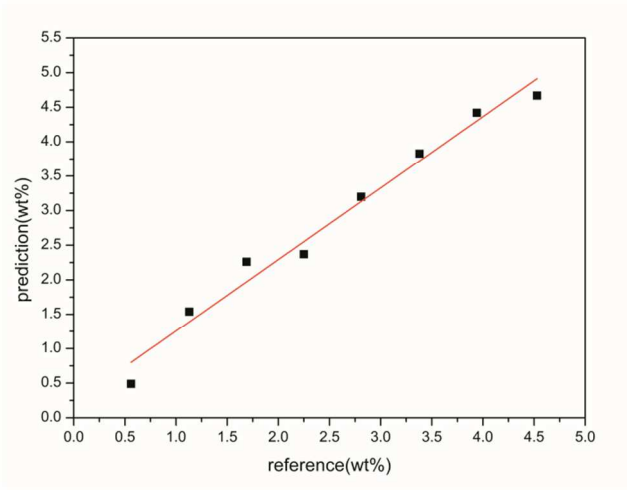

Fig. 7. Relationship of the predictive values with the reference values for the water of crystallization content. The straight line is obtained by linear regression.

4 Conclusion

Near infrared spectroscopy is a promising technique as it is a rapid and non-destructive method. The result of the study shows that the NIR model for the water of crystallization content of dihydrate gypsum can be used to detect the rocks of Yungang Grottoes in situ. In the archaeological site, the spectra of the actual samples can be recorded by the portable FTNIR spectrometer. Then the water of crystallization content of dihydrate gypsum can be obtained by importing the NIR spectroscopy into the NIR model. Therefore, the determination of the water of crystallization will only need the portable FTNIR instrument and a laptop in the future. It may be proved to be a valid,

simple and fast tool to reduce analytical cost. The water of crystallization content obtained by the NIR model can be applied to evaluate the degree of weathering of rocks. Based on the above work, the protection and restoration of Yungang Grottoes can be carried out.

Acknowledgments

This work is supported by the National Basic Research Program of China (973 Program) (2012CB725300) and the National Science and Technology Support Program (2009BAK53B01).

Notes and references

1. C. S. Christoforou, L. G. Salmon and G. R. Cass, Air exchange within the Buddhist cave temples at Yungang, China, *Atmos. Environ.*, 1996, **30**, 3995-4006.
2. R. Z. Liu, B. J. Zhang, H. Zhang and M. F. Shi, Deterioration of Yungang Grottoes: Diagnosis and research, *J. Cult. Herit.*, 2011, **12**, 494-499.
3. L. G. Salmon, C. S. Christoforou and G. R. Cass, Airborne Pollutants in the Buddhist Cave Temples at the Yungang Grottoes, China, *Environ. Sci. Technol.*, 1994, **28**, 805-811.
4. H. Böke, E. H. Göktürk, E. N. Caner-Saltık and Ş. Demirci, Effect of airborne particle on SO2–calcite reaction, *Appl. Surf. Sci.*, 1999, **140**, 70-82.
5. H. Böke, E. H. Hale Göktürk and E. N. Caner Saltık, Effect of some surfactants on SO2–marble reaction, *Mater. Lett.*, 2002, **57**, 935-939.
6. S. B. Ziegenbalg, C. Berthold, A. Kappler and J. Peckmann, Gypsum whiskers in Messinian evaporites identified by mu-XRD2, *Facies*, 2011, **57**, 249-253.
7. J. Adamovic, R. Mikulas, J. Schweigstillova and V. Bohmova, Porosity changes induced by salt weathering of sandstones, Bohemian Cretaceous Basin, Czech Republic, *Acta Geodyn. Geomater.*, 2011, 8, 29-45.
8. O. Artieda, Morphology and micro-fabrics of weathering features on gyprock exposures in a semiarid environment (Ebro Tertiary Basin, NE Spain), *Geomorphology*, 2013, **196**, 198-210.
9. B. Burkart, G. C. Goss and J. P. Kern, The role of gypsum in production of sulfate-induced deformation of lime-stabilized soils, *Environ. Eng. Geosci.*, 1999, **5**, 173-187.
10. C. Butscher, P. Huggenberger, E. Zechner and H. H. Einstein, Relation between hydrogeological setting and swelling potential of clay-sulfate rocks in tunneling, *Eng. Geol.*, 2011, **122**, 204-214.
11. J. S. Sanchez, C. A. S. Alves, J. R. V. Romani and D. F. Mosquera, Origin of Gypsum-rich Coatings on Historic Buildings, *Water Air Soil Pollut.*, 2009, **204**, 53-68.
12. Z. Varilova, R. Prikryl and V. Cilek, Pravcice Rock Arch (Bohemian Switzerland National Park, Czech Republic) deterioration due to natural and anthropogenic weathering, *Environ. Earth Sci.*, 2011, **63**, 1861-1878.
13. F. Gogé, R. Joffre, C. Jolivet, I. Ross and L. Ranjard, Optimization criteria in sample selection step of local regression for quantitative analysis of large soil NIRS database, *Chemometr. Intell. Lab.*, 2012, **110**, 168-176.
14. Q. J. Han, H. L. Wu, C. B. Cai, L. J. Tang and R. Q. Yu, Using near-infrared spectroscopy and differential adsorption bed method to study adsorption kinetics of

orthoxylene on silica gel, *Talanta*, 2008, **76**, 752-757.

15. M. Ito, T. Suzuki, S. Yada, A. Kusai, H. Nakagami, E. Yonemochi and K. Terada, Development of a method for the determination of caffeine anhydrate in various designed intact tables by near-infrared spectroscopy: A comparison between reflectance and transmittance technique, *J. Pharm. Biomed. Anal.*, 2008, **47**, 819-827.
16. N. Labbe, S. H. Lee, H. W. Cho, M. K. Jeong and N. Andre, Enhanced discrimination and calibration of biomass NIR spectral data using non-linear kernel methods, *Bioresour. Technol.*, 2008, **99**, 8445-8452.
17. A. M. K. Pedro and M. M. C. Ferreira, Nondestructive determination of solids and carotenoids in tomato products by near-infrared spectroscopy and multivariate calibration, *Anal. Chem.*, 2005, **77**, 2505-2511.
18. M. Bala and M. Singh, Non destructive estimation of total phenol and crude fiber content in intact seeds of rapeseed-mustard using FTNIR, *Ind. Crop. Prod.*, 2013, **42**, 357-362.
19. D. Cozzolino, W. Cynkar, N. Shah and P. Smith, Quantitative analysis of minerals and electric conductivity of red grape homogenates by near infrared reflectance spectroscopy, *Comput. Electron. Agr.*, 2011, **77**, 81-85.
20. A. Alishahi, H. Farahmand, N. Prieto and D. Cozzolino, Identification of transgenic foods using NIR spectroscopy: A review, *Spectroc. Acta Pt. A-Molec. Biomolec. Spectr.*, 2010, **75**, 1-7.
21. M. B. Whitworth, S. J. Millar and A. Chau, Food quality assessment by NIR hyperspectral imaging, *Sensing for Agriculture and Food Quality and Safety Ii*, 2010, **7676**, 12.
22. Y. Wang, X. Ma, Y. D. Wen, C. X. Yu, L. P. Wang, L. L. Zhao and J. H. Li, Tobacco Quality Analysis of Producing Areas of Yunnan Tobacco Using Near-Infrared (NIR) Spectrum, *Spectrosc. Spectr. Anal.*, 2013, **33**, 78-80.
23. Y. Zhang, Q. Cong, Y. F. Xie, J. X. Yang and B. Zhao, Quantitative analysis of routine chemical constituents in tobacco by near-infrared spectroscopy and support vector machine, *Spectroc. Acta Pt. A-Molec. Biomolec. Spectr.*, 2008, **71**, 1408-1413.
24. H. Jiang, G. H. Liu, C. L. Mei and Q. S. Chen, Qualitative and quantitative analysis in solid-state fermentation of protein feed by FT-NIR spectroscopy integrated with multivariate data analysis, *Anal. Methods*, 2013, **5**, 1872-1880.
25. M. C. A. Marcelo, C. A. Martins, D. Pozebon and M. F. Ferrao, Methods of multivariate analysis of NIR reflectance spectra for classification of yerba mate, *Anal. Methods*, 2014, **6**, 7621-7627.
26. X. Zhao, Q. B. Zhu, M. Huang and H. Y. Cen, An IGA-PLSP method for FT-NIR wavelength selection for measuring soluble solid content of citrus fruits, *Anal. Methods*, 2013, **5**, 4811-4817.

27. Y. Dou, F. P. Qiu, P. Y. Liu, Y. Q. Ren and Y. L. Ren, Nondestructive quantitative analysis of paracetamol tablet medicines by NIR spectroscopy, *Chem. J. Chin. Univ.-Chin.*, 2004, **25**, 53-55.
28. P. Li, G. Du, W. Cai and X. Shao, Rapid and nondestructive analysis of pharmaceutical products using near-infrared diffuse reflectance spectroscopy, *J. Pharmaceut. Biomed.*, 2012, **70**, 288-294.
29. Y. Yang, O. O. Soyemi, P. J. Scott, M. R. Landry, S. M. C. Lee, L. Stroud and B. R. Soller, Quantitative measurement of muscle oxygen saturation without influence from skin and fat using continuous-wave near infrared spectroscopy, *Opt. Express*, 2007, **15**, 13715-13730.
30. G. Zonios and A. Dimou, Modeling diffuse reflectance from semi-infinite turbid media: application to the study of skin optical properties, *Opt. Express*, 2006, **14**, 8661-8674.
31. D. Baykal, O. Irrechukwu, P. C. Lin, K. Fritton, R. G. Spencer and N. Pleshko, Nondestructive Assessment of Engineered Cartilage Constructs Using Near-Infrared Spectroscopy, *Appl. Spectrosc.*, 2010, **64**, 1160-1166.
32. S. Laske, M. Kracalik, M. Feuchter, G. Pinter, G. Maier, W. Marzinger, M. Haberkorn and G. R. Langecker, FT-NIR as a Determination Method for Reinforcement of Polymer Nanocomposites, *J. Appl. Polym. Sci.*, 2009, **114**, 2488-2496.
33. D. D. S. Fernandes, A. A. Gomes, G. B. da Costa, G. W. B. da Silva and G. Veras, Determination of biodiesel content in biodiesel/diesel blends using NIR and visible spectroscopy with variable selection, *Talanta*, 2011, **87**, 30-34.
34. E. D. Gaiao, S. R. B. dos Santos, V. B. dos Santos, E. C. L. do Nascimento, R. S. Lima and M. C. U. de Araujo, An inexpensive, portable and microcontrolled near infrared LED-photometer for screening analysis of gasoline, *Talanta*, 2008, **75**, 792-796.
35. P. J. Gemperline, Rugged spectroscopic calibration for process control, *Chemometr. Intell. Lab.*, 1997, **39**, 29-40.
36. P. Vandenabeele, R. Garcia-Moreno, F. Mathis, K. Leterme, E. Van Elslande, F.-P. Hocquet, S. Rakkaa, D. Laboury, L. Moens, D. Strivay and M. Hartwig, Multi-disciplinary investigation of the tomb of Menna (TT69), Theban Necropolis, Egypt, *Spectrochim. Acta A.*, 2009, **73**, 546-552.
37. M. Vagnini, C. Miliani, L. Cartechini, P. Rocchi, B. G. Brunetti and A. Sgamellotti, FT-NIR spectroscopy for non-invasive identification of natural polymers and resins in easel paintings, *Anal. Bioanal. Chem.*, 2009, **395**, 2107-2118.